A set-membership approach for high integrity height-aided satellite positioning

Vincent Drevelle, Philippe Bonnifait

A set-membership approach for high integrity height-aided satellite positioning

Vincent Drevelle, Philippe Bonnifait

Heudiasyc
CNRS: UMR 6599 – Université de Technologie de Compiègne
Centre de Recherche de Royallieu, BP 20529, 60205 Compiègne, France

Tel. +33 3 44 23 46 45
Fax. +33 3 44 23 44 77
Email: vincent.drevelle@hds.utc.fr

The final publication is available at www.springerlink.com:
http://dx.doi.org/10.1007/s10291-010-0195-3

Abstract A *Robust Set Inversion via Interval Analysis* method in a bounded error framework is used to compute three-dimensional location zones in real time, at a given confidence level. This approach differs significantly from the usual Gaussian error model paradigm, since the satellite positions and the pseudorange measurements are represented by intervals encompassing the true value with a particular level of confidence. The method computes a location zone recursively, using contractions and bisections of an arbitrarily large initial location box. Such an approach can also handle an arbitrary number of erroneous measurements using a q-relaxed solver, and allows the integration of geographic and cartographic information such as digital elevation models or 3-dimensional maps. With enough data redundancy, inconsistent measurements can be detected and even rejected. The integrity risk of the location zone comes only from the measurement bounds settings, since the solver is guaranteed. A method for setting these bounds for a particular location zone confidence level is proposed. An experimental validation using real L1 code measurements and a digital elevation model is also reported in order to illustrate the performance of the method on real data.

Keywords: *GPS; Interval Analysis; Robust positioning; Elevation model; Land vehicles*

Introduction

Positioning services are becoming more frequently used in safety- and reliability-critical applications for land vehicles, where not only an estimate of a user's location is required, but also confidence indicators and means of ensuring integrity.

Fig. 1 Experimental intelligent vehicles: Carmen and Strada

In the context of urban navigation with Global Navigation Satellite Systems (GNSS), the main source of erroneous measurements is multipath propagation and more specifically non-line-of-sight propagation, when the direct signal is blocked by buildings and only reflected signals are observed. Furthermore, several multipath altered measurements can be observed at the same epoch (Le Marchand et al. 2009). Satellite-Based Augmentation Systems (SBAS) have little effect in these conditions since they provide integrity information to protect the user against signal-in-space malfunction, but not against local effects of multipath. Moreover, satellite outages due to signal blocking by surrounding buildings have other significant effects such as reducing data redundancy, degrading the geometrical configuration, and decreasing SBAS availability. Other sources of information are necessary to increase information redundancy and improve localization in such difficult environment. The usual approach is to use proprioceptive sensors that enable dead reckoning, the drift of which is compensated by the available GNSS measurements. For land vehicles, an alternative approach is to make use of geographical information to constrain the location on mapped roads (Fouque and Bonnifait 2008). Another source of information can be a Digital Elevation Model (DEM), which is very useful for constraining the altitude (Li et al. 2005).

In practice, the knowledge of positioning accuracy is crucial. Localization can thus be directly addressed as a set-membership problem that consists in finding the zone in which the user is located, with a given level of confidence. Set-theoretical methods have successfully been employed in robotics to address localization problems (Jaulin et al. 2002; Meizel et al. 2002). These methods have interesting properties, such as the ability to handle several hypotheses in cases of ambiguous solutions simply by computing disconnected solution sets. Moreover, when measurement errors are bounded, guaranteed solutions can be computed — i.e. location zones in which the user is guaranteed to be located. In practice, finding absolute bounds for the error is not always possible, and is often an excessively conservative approach that fails to yield informative solutions. We use a relaxed set-membership approach, which allows a given number of measurements to be treated as outliers without affecting the consistency of the solution set. This enables dealing with erroneous measurements, while avoiding empty solutions. The solution-set integrity risk is bounded by the risk taken when setting measurement error bounds and the number of tolerated outliers. No risk is added by the employed set inversion algorithm, which solves the problem in a guaranteed way. This makes the method particularly attractive in comparison with existing solvers. Another advantage of a set-membership approach is that it allows geographical information to be incorporated easily. Spatial inequality constraints can be introduced into the computation without biasing the estimation process.

After a brief overview of current GPS integrity approaches, we introduce the concept of set-membership positioning with a simple two-dimensional pedagogical example. Guaranteed solvers for set-inversion based on interval analysis and constraint propagation are then presented. A robust solver is also introduced, and a method for setting measurement error bounds in relation to a specified risk is explained. Finally, experimental results using real L1 GPS pseudorange measurements and a DEM are presented and analyzed.

Current approaches

Punctual GNSS positioning using pseudoranges is typically handled as a nonlinear Least-Squares problem using a Gauss-like method (Leick 2004; Kaplan and Hegarty 2006). Other methods have been proposed to provide a non-iterative computation (Bancroft 1985) or to allow positioning in situations with fewer than four good measurements (Chang et al. 2009). In practice, some means of computing an upper bound of the positioning error, linked to an integrity risk, is required to determine whether the navigation system is usable for a given task. When dealing with safety applications, the system should be able to handle erroneous measurements. The concepts of internal and external reliability (Baarda 1968) enable to quantify the system's response in the presence of an unmodeled error.

Internal reliability is characterized by the Minimal Detectable Bias (MDB), which represents the size of the errors that can be detected by a given test statistics (Salzmann 1991). The null hypothesis H_0 represents the fault free case, where model errors are absent. The alternative hypothesis H_a considers the existence of a bias in one of the measurements. The MDB depends not only on the level of confidence and on the detection power of the test statistics, but also on the geometry of the problem, the noise model and the alternate hypothesis considered.

External reliability characterizes the effect in the position domain of an undetected error model. Several external reliability metrics have been defined, such as the Bias to Noise Ratio, which represents the significance of such an unobserved error in a normalized way, and the Horizontal and Vertical Protection Levels (HPL/VPL).

The Detection, Identification and Adaptation (DIA) scheme proposed in Teunissen (1990) enables quality control of the position solution, in parallel to a

Kalman filter. Error detection is first performed by testing H_0 against H_a. Then, if a fault is detected, a second test statistics is used to identify the alternate hypothesis, if possible. Upon success, an adaptation procedure is done to take into account the detection. The chosen alternative hypotheses H_a are often limited to errors on single measurements. The processing of simultaneous faults is performed by iteratively applying DIA until H_0 is validated.

Aviation receivers need to provide HPL and VPL that define, within an integrity risk, the statistical upper bounds of position errors that will not be exceeded without being detected in a given time to alert. This is achieved by Receiver Autonomous Integrity Monitoring (RAIM) (Brown 1992; Walter and Enge 1995; Feng et al. 2006), which implements a local version of the DIA scheme on single epochs, called Fault Detection and Exclusion (FDE). The thresholds of the test statistics used are set to meet the required navigation performance specifications on integrity and availability. RAIM can be improved by the use of a dynamic model (Hewitson 2007).

Other methods to compute navigation solutions in the presence of erroneous measurements are based on robust estimation, like Huber's robust M-estimator (Huber 1964). Range Consensus (Schroth et al. 2008) is an approach which computes solutions on random four-satellite subsets and retains the solution which is compatible with the most measurements, while rejecting the other measurements as outliers. Solution separation is another method, which consists in computing a solution with all available measurements, and all the sub-solutions excluding one measurement (Schubert 2006).

A way to reduce the Minimal Detectable Biases, and as a consequence improving integrity, is to add external information like a barometric pressure sensor for instance (Gutmann et al. 2009). For ground vehicles, altitude information can be provided to the system by using a DEM. This information is often added as a virtual range from the center of the earth. In our approach, the altitude information is easily introduced as a *constraint* coming from a DEM.

Set-membership positioning

In a bounded-error context, determining the user location zone consists in finding the set of positions compatible with the measurements and their associated error bounds. Positioning as a set-membership problem is introduced here with a simple 2D localization example, also showing the effects of wrong measurements on the solution-set. In the presence of outliers, a relaxed approach enables robust set-membership positioning.

Motivation

Algorithms that compute position from measurements for snapshot problems are often based on punctual iterative methods that can be made robust to erroneous measurements. Their main drawback is the risk to fall into a local minimum if the initial guess is too far from the solution, or if erroneous measurements are not properly handled.

Set-inversion methods guarantee that no solution will be missed inside an arbitrarily big initial box, even if the equations are nonlinear. Relaxed-set inversion is an extension that can also compute a guaranteed solution in the presence of several outliers. When considering single faults, 1-relaxed set-inversion provides external reliability information by computing the solution set assuming the hypothesis of at most one erroneous measurement. In other words, the solution set computed with the 1-relaxed solver covers the hypotheses H_0 and H_a.

For the DIA method, H_0 is tested by a statistical test on the residuals. Identification is then done using individual tests on each H_a. Transition from internal integrity to external reliability assumes a linear(ized) model and usually one fault at a time. A set-inversion method can handle nonlinear models without adding any risk of invalid linearization. Such an approach can also be robust to an arbitrary number of outliers, under the hypothesis that there is enough redundancy. Therefore, robust set-inversion allows specifying alternate hypotheses H_a with several simultaneous faults without explicitly testing every fault combination.

Finally, when the problem is under-constrained, a set-inversion method can compute all the location sets, even if there is a manifold of solutions. This is particularly difficult to achieve using the approaches mentioned above. For instance, with only 4 satellites in view, a location zone robust to one erroneous measurement can still be computed.

Illustrative example with static beacons

Let us consider a time-of-flight positioning example having similarities with GNSS even if, thanks to the longer ranges involved, nonlinearity is not a difficult problem for GNSS positioning. One robot and three beacons communicate via a radio link, as in Röhrig and Müller (2009). This radio link not only allows communication, but also precision ranging with 1m accuracy.

To perform set-membership positioning, each measurement has to be represented as the set of possible values given uncertainty. Intervals are commonly used to express measurement inaccuracy. The maximum expected ranging error is added to the measured value to represent measurements as intervals

$$[d^i] = [d^i - e_{max}, d^i + e_{max}] \qquad (1)$$

Each measurement acts as a constraint on the robot's location, setting bounds on the distance between the robot and the beacon. Since the robot and the beacons lie on the same horizontal plane, we have the membership relation:

$$\sqrt{(x_R - x_{B^i})^2 + (y_R - y_{B^i})^2} \in [d^i] \qquad (2)$$

Given (2), each measurement constrains the robot location inside a ring, whose inner and outer radii are respectively the lower and upper bounds of the measurement interval $[d^i]$.

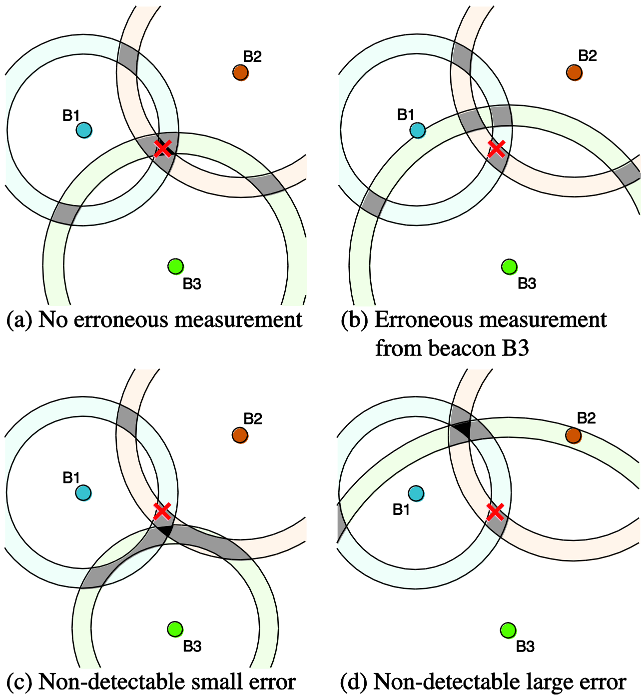

Fig. 2 Localization using 3 beacons. Solution set in black. 1-relaxed solution set in black and grey. The actual solution is shown as a red cross.

As there are three beacons, the measurement equation must be satisfied for the three measurements. The robot is thus located within the intersection of the three rings (the black area in Fig. 2a).

It is important to bear in mind that as long as the measurements are consistent with the chosen bounded error model, the solution set will include the true user location.

Effect of wrong measurements

Beacon ranging can be affected by multipath propagation or faulty beacons, so that a measured range may be inconsistent with the error bounds. This kind of measurement is often referred to as an "outlier" or a "fault". When using standard set inversion, there are two possible consequences:

- The solution is the empty set (Fig. 2b). This occurs when the erroneous measurement is inconsistent with the other measurements, so that there is no common intersection. One may therefore immediately conclude that there is something wrong with the measurements or with the model.

- The solution is not empty, but does not contain the actual robot location (Fig. 2c and 2d). The set-membership method is then unable to detect the presence of an erroneous measurement, and the solution set is inconsistent with the truth.

To deal with erroneous measurements, a robust set-membership method must be used. This is done by relaxing the number of constraints to be satisfied. In this example, allowing at most one erroneous measurement is achieved by considering the set of solutions compatible with at least two measurements (the gray and black surfaces in Fig. 2). In the general case, an arbitrary number q of erroneous measurements can be tolerated, using the q-relaxed intersection of the constraints (Jaulin 2009).

Set inversion via interval analysis

In the previous example, the solution sets for each constraint were easy to represent as rings, and we assumed that any set could be computed with an exact representation. In real localization problems, the constraints are given by the measurements and an observation function, but they may also reflect prior information like the terrain profile, which can lead to arbitrary sets of solutions. We therefore use interval analysis (Moore 1966) to perform a guaranteed set inversion.

Interval analysis

Since an exact representation of sets is not tractable in the general case, an efficient and easily implemented representation is to consider intervals, and their multidimensional extension: *interval vectors*, also called *boxes*. Let $\mathbf{IR}$ be the set of real intervals, and $\mathbf{IR}^n$ the set of n-dimensional boxes.

Computations can easily be performed on intervals, thanks to interval arithmetic. *Inclusion functions* $[\mathbf{f}]$ are defined such that the image of $[\mathbf{x}]$ by $[\mathbf{f}]$ includes the image of $[\mathbf{x}]$ by $\mathbf{f}$:

$$\forall[\mathbf{x}]\in\mathbf{IR}^n, \mathbf{f}([\mathbf{x}])\subset[\mathbf{f}]([\mathbf{x}]).$$

To approximate compact sets in a guaranteed way, *subpavings* are used. A subpaving of a box $[\mathbf{x}]$ is the union of nonempty and non-overlapping subboxes of $[\mathbf{x}]$. A guaranteed approximation of a compact set $\mathbf{X}$ can be made by bracketing it between an inner subpaving $\underline{\mathbf{X}}$ and an outer subpaving $\overline{\mathbf{X}}$ such as $\underline{\mathbf{X}}\subset\mathbf{X}\subset\overline{\mathbf{X}}$ (Fig. 3).

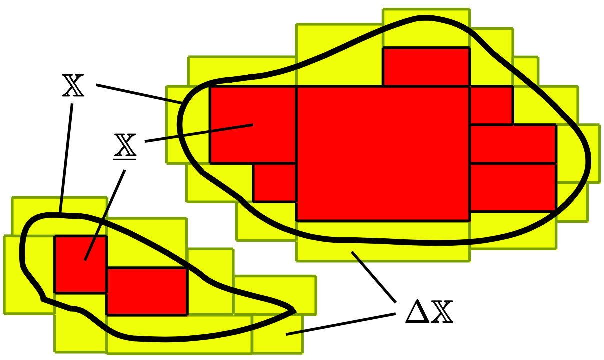

Fig. 3 Bracketing of the hatched set between two subpavings. *Red boxes: inner subpaving* $\underline{\mathbf{X}}$, *Red and yellow: outer subpaving* $\overline{\mathbf{X}}=\underline{\mathbf{X}}\cup\Delta\mathbf{X}$

Set inversion

The set inversion problem consists in determining the set $\mathbf{X}$ such as $\mathbf{f}(\mathbf{X}) = \mathbf{Y}$ when $\mathbf{Y}$ is known. A box $[\mathbf{x}]$ of $\mathbf{IR}^n$ is said to be *feasible* if $[\mathbf{x}] \subset \mathbf{X}$ (all elements of the box are solutions of the problem) and *unfeasible* if $[\mathbf{x}] \cap \mathbf{X} = \emptyset$ (none of the elements of the box is a solution of the problem), otherwise $[\mathbf{x}]$ is ambiguous. We can characterize the feasibility of boxes by using an *inclusion function* $[\mathbf{f}]$ of the function $\mathbf{f}$ to be inverted,

- If $[\mathbf{f}]([\mathbf{x}]) \subset \mathbf{Y}$ then $[\mathbf{x}]$ is feasible
- If $[\mathbf{f}]([\mathbf{x}]) \cap \mathbf{Y} = \emptyset$ then $[\mathbf{x}]$ is unfeasible
- Else $[\mathbf{x}]$ is indeterminate, meaning it can be feasible, unfeasible or ambiguous.

Starting from an arbitrarily large prior searching box $[\mathbf{x}_0]$, the *Set Inversion Via Interval Analysis* (SIVIA) algorithm (Jaulin and Walter 1993) works by testing the feasibility of boxes. Feasible boxes are added to the inner subpaving $\underline{\mathbf{X}}$ of solutions. Unfeasible boxes are discarded, since they contain no solution. Finally, indeterminate boxes are bisected into two subboxes, which are enqueued in the list L of boxes waiting to be examined. Algorithm termination is ensured by adding indeterminate boxes whose width is less than ε to the subpaving of indeterminate boxes $\Delta\mathbf{X}$. Thus the outer subpaving is $\overline{\mathbf{X}} = \underline{\mathbf{X}} \cup \Delta\mathbf{X}$.

The number of bisections required gets exponentially larger as the dimension of the problem increases, and the computational burden quickly becomes intractable. To counteract the curse of dimensionality, *contractors* have to be used (Jaulin et al. 2001b). A contractor is a function that shrinks a box without losing any solutions. It can speed up computation without sacrificing the guarantee of a solution. A simple way to build a contractor is to use a constraint propagation algorithm (Jaulin et al. 2001b).

q-relaxed set inversion

Robustness can be implemented by relaxing a given number q of constraints involving outliers. The solver will then compute a subpaving of the state space consistent with at least $m-q$ measurements, where m is the length of the observation vector. This is done using the so called q*-relaxed intersection*.

Considering m sets $\mathbf{X}_1,\ldots,\mathbf{X}_m$ of $\mathbf{R}^n$, the q-relaxed intersection $\bigcap^{\{q\}} \mathbf{X}_i$ is the set of $\mathbf{x} \in \mathbf{R}^n$ which belong to at least $m-q$ of the $\mathbf{X}_i$'s. The *Robust Set Inverter via Interval Analysis* (RSIVIA) solver (Jaulin et al. 2001b) guarantees the computation of a q-relaxed solution set (see Algorithm 1).

Algorithm 1 RSIVIA (in: $[\mathbf{x}_0]$, $\mathbf{f}$, $\mathbf{Y}$, q)
Robust Set Inverter via Interval Analysis

$\text{push}([\mathbf{x_0}], \mathsf{L})$
while $\mathsf{L} \neq \emptyset$ **do**
  $[\mathbf{x}] = \text{pull}(\mathsf{L})$
  repeat
    for $i = 1 \ldots m$ **do**
      $[\mathbf{x}](i)$ = contract $[\mathbf{x}]$ with f_i and $[y_i]$
    end for
    $$[\mathbf{x}] = \left[\bigcap_{i \in \{1,\ldots,m\}}^{\{q\}} [\mathbf{x}](i) \right]$$
    // hull of the q-relaxed intersection of m boxes
  until no more contraction can be done on $[\mathbf{x}]$
  if $[\mathbf{x}] \neq \emptyset$ **then**
    $([\mathbf{x_1}], [\mathbf{x_2}]) = \text{bisect}([\mathbf{x}])$
    $\text{push}([\mathbf{x_1}], \mathsf{L}); \text{push}([\mathbf{x_2}], \mathsf{L})$
  end if
end while
return L

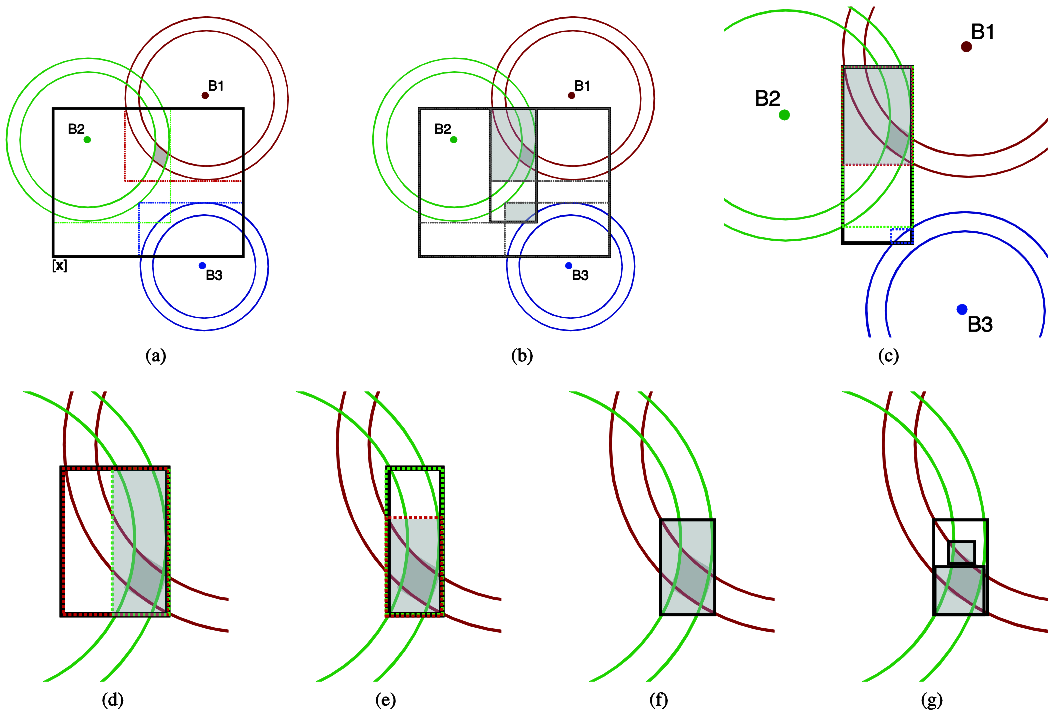

Fig. 4 Steps of RSIVIA on a 3 beacon localization problem

Fig. 4 shows the main steps of RSIVIA, applied to a fixed beacon localization problem. The prior box is first contracted independently with each measurement to get three boxes approximating the intersection of each constraint with the prior box (Fig. 4a). The grayed zones in Fig. 4b represent the 1-relaxed intersections of the three boxes. The hatched box, which is the box union of the grayed boxes, becomes a new initial box. We have thus contracted the initial box without losing any solutions. Contraction with each measurement is repeated, starting with the new box (Fig. 4c), following which the initial box is reduced again so as to enclose the q-relaxed intersection of contracted boxes. These steps are repeated (Fig. 4d and 4e) until no further contractions can be performed (Fig. 4f). A bisection is then carried out, and the contraction process is applied to the two subboxes (Fig. 4g).

Setting measurement error bounds as a function of a given level of confidence

When using a q-relaxed guaranteed solver such as RSIVIA, the probability of the true solution being inside the computed solution set can be computed, given a prior measurement error distribution and a maximum number of outliers (denoted q) (Drevelle and Bonnifait 2009b). The risk is taken when setting measurement error bounds and the maximum number of outliers. The bounds are then propagated in a guaranteed way, such that no risk is added by the solver when set-inversion is performed.

Knowing the probability density function f_{e_y} of the measurement error e_y and the error bounds $[a,b]$, a measurement y_{meas} is represented by the interval $[y_{meas}] = [y_{meas} + a, y_{meas} + b]$. The probability $p = P(y \in [y_{meas}])$ of the true y being inside $[y_{meas}]$ can be computed.

$$p = P(y \in [y_{meas}]) = \int_a^b f_{e_y}(\alpha) d\alpha \qquad (3)$$

Let n_{ok} be the number of measurements that respect the error bounds. Given the assumption of independence, the probability of having exactly k correct measurements out of m is given by the binomial law:

$$P(n_{ok} = k) = \frac{m!}{k!(m-k)!} p^k (1-p)^{m-k} \qquad (4)$$

Thus, by summing (4) over successive k values, the probability of having at least $m-q$ correct measurements is

$$P(n_{ok} \geq m-q) = \sum_{k=m-q}^{m} \frac{m!}{k!(m-k)!} p^k (1-p)^{m-k} \qquad (5)$$

A guaranteed algorithm like RSIVIA computes a conservative approximation $\overline{\mathbf{X}}$ of the solution set $\mathbf{X}$. Moreover, if the hypotheses made on the measurements are confirmed, the solution set is consistent with the truth. Thus,

$$n_{ok} \geq m-q \Rightarrow x \in \mathbf{X} \Rightarrow x \in \overline{\mathbf{X}}$$

which leads to

$$P(x \in \overline{\mathbf{X}}) \geq P(x \in \mathbf{X}) \geq P(n_{ok} \geq m-q) \qquad (6)$$

Setting $P(n_{ok} \geq m-q)$ to a confidence level P_{conf} will ensure at least this confidence level for the computed solution. Since the number of measurements m and the number of tolerated outliers q are known, p can be determined from (5) for a given $P(n_{ok} \geq m-q)$. Measurement bounds can then be chosen to satisfy (3).

There is one degree of freedom left for choosing the lower and upper bounds a and b of the measurement error interval. Consequently, they may be chosen to minimize the width of $[a,b]$, *i.e.* minimize $b-a$.

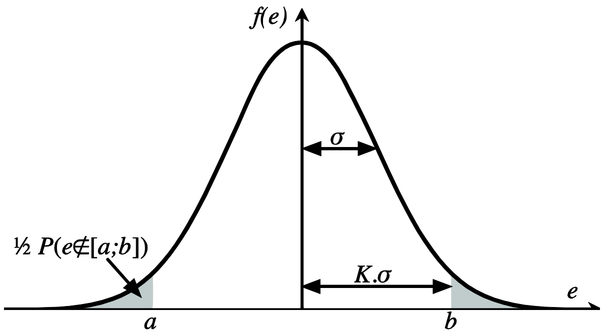

Fig. 5 Setting bounds on a Gaussian measurement error

In the case of a centered Gaussian measurement error $e_y \sim N(0,\sigma_y)$, which is the usual model in GPS positioning, with Φ representing the cumulative distribution function of the standard normal distribution, the measurement interval should be set to

$$[y_{meas}] = [y_{meas} - K\sigma_y, y_{meas} + K\sigma_y] \quad (7)$$

In this case, K is simply given by

$$K = -\Phi^{-1}\left(\frac{1-p}{2}\right) \qquad (8)$$

This way, the same amount of risk is taken on each tail of the Gaussian distribution of error (Fig. 5).

Computation of GPS location zones

The set-inversion methods presented above are applied to GPS pseudorange measurements in this section. It enables computing location zones in real time, and performing fault detection and identification.

Set-membership GPS localization

GPS positioning with pseudoranges is a four-dimensional problem: along with the Cartesian coordinates (x, y, z) of the user, the user's clock offset dt_u has to be estimated. With ρ_i being the corrected pseudoranges, the GPS code observation model in Earth Centered Earth Fixed (ECEF) coordinates is (for simplification, the time index is omitted in the following equations):

$$\begin{pmatrix} \rho_1 \\ \rho_2 \\ \vdots \\ \rho_m \end{pmatrix} = \begin{pmatrix} \sqrt{(x-x_1^s)^2+(y-y_1^s)^2+(z-z_1^s)^2}+cdt_u \\ \sqrt{(x-x_2^s)^2+(y-y_2^s)^2+(z-z_2^s)^2}+cdt_u \\ \vdots \\ \sqrt{(x-x_m^s)^2+(y-y_m^s)^2+(z-z_m^s)^2}+cdt_u \end{pmatrix}$$

Satellite positions at the emission time (x_i^s, y_i^s, z_i^s) are known only with uncertainty, owing to the inaccuracy of the broadcast ephemeris information. Using interval analysis, it is easy to take this inaccuracy into account. For each satellite, we consider a box $[\mathbf{x}_i^s] = ([x_i^s],[y_i^s],[z_i^s])$ whose bounds are chosen to contain the true satellite position at a given confidence level.

Pseudorange corrections are imprecise because of model and parameter errors. Moreover, the receiver is also subject to measurement errors. We therefore model the corrected pseudorange measurements as intervals $[\rho_i]$ whose bounds are determined given an integrity risk.

The location zone computation consists in characterizing the set $\mathbf{X}$ of all locations compatible with the measurements and the satellite position intervals:

$$\begin{aligned} \mathbf{X} = \ & \{(x,y,z,cdt_u) \in \mathbf{R}^4 \mid \forall i = 1\ldots m, \\ & \exists \rho_i \in [\rho_i], \exists (x_i^s, y_i^s, z_i^s) \in [\mathbf{x}_i^s], \\ & \rho_i = \sqrt{(x-x_i^s)^2 + (y-y_i^s)^2 + (x-y_i^s)^2} + cdt_u\} \end{aligned}$$

The solution set is the set of locations for which a pseudorange and a satellite position can be found inside the measurement and satellite position intervals for every satellite.

To add robustness, the location zone is computed assuming at least $m-1$ good measurements. RSIVIA is used to solve the relaxed set inversion problem. By recursively contracting and bisecting an arbitrarily large initial box, this algorithm returns a subpaving of the state-space (user position and clock offset) guaranteed to include the solution set, i.e. an outer approximation of the solution set by a set of boxes. As long as the initial hypothesis is valid, i.e. as long as only at most one measurement exceeds the error bounds, the true receiver position is guaranteed to be inside the computed localization zone. The bounds are chosen so that the risk of more than one wrong measurement, i.e. the risk that at least two measurements do not respect the error bounds, is 10^{-7}.

The constraint induced by the i^{th} pseudorange measurement is represented by the natural inclusion function of the observation function:

$$[f_i]([\mathbf{x}]) = \sqrt{([x]-[x_i^s])^2 + ([y]-[y_i^s])^2 + ([z]-[z_i^s])^2} + c[dt_u] \qquad (9)$$

A constraint propagation contractor for (9) is built using the Fall-Climb algorithm (Jaulin et al. 2001a), which allows constraints to be propagated in an optimal order.

GPS-only location zone computation

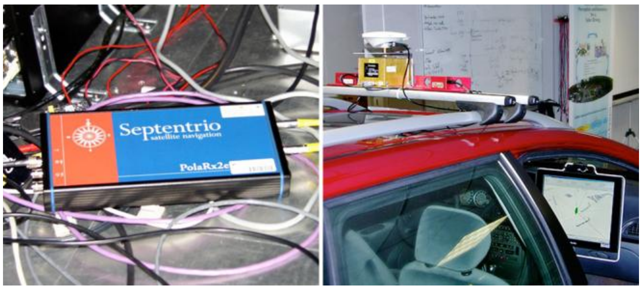

Fig. 6 Experimental setup. *Left:* Septentrio PolaRx GPS Receiver. *Right:* Experimental vehicle running the real-time set-membership positioning application, GPS antenna on the roof.

Test data were recorded using a *Septentrio PolaRx* receiver and the experimental vehicle shown in Fig. 6. The ground truth solution is provided by a post-processed *Trimble 5700* receiver with a local base. The sequence covers 1800 m of road network near the lab in Compiègne, and lasts about 170 seconds. During this test, the number of used L1-pseudoranges was between 4 and 6. Figure 7 shows the bounding boxes of solutions for each measurement epoch. These solutions are computed using a nonrobust SIVIA.

The EGNOS augmentation system has been used to get corrected pseudoranges with associated measurement error variances, assuming an overbounding Gaussian distribution.

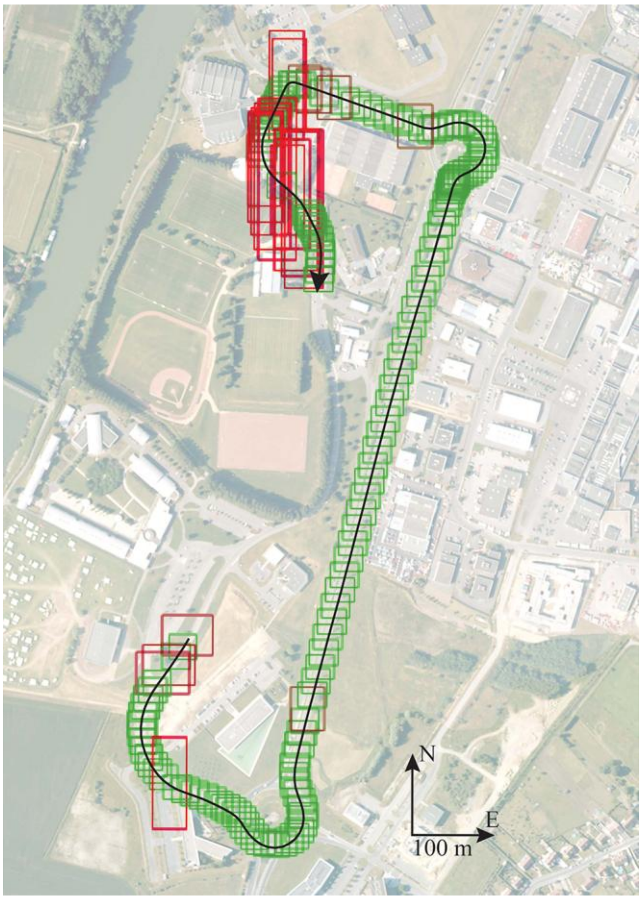

Fig. 7 Bird's eye view of the trajectory. Boxes are bounding boxes of nonrobust solution sets. Reference trajectory is in black.

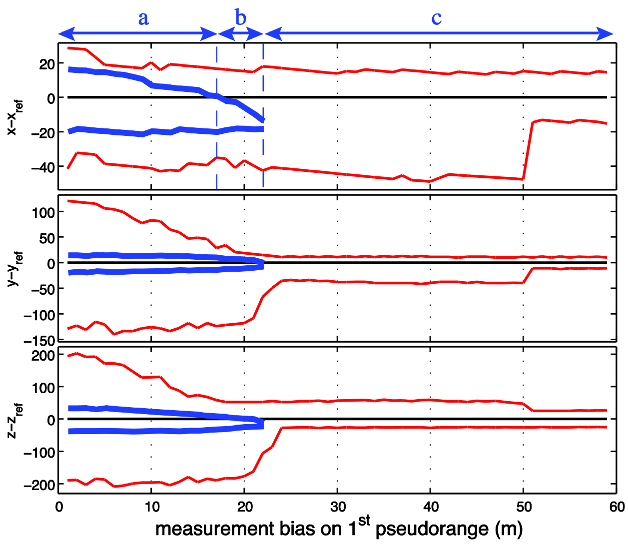

Fig. 8 Location zone bounds with respect to ground truth. An increasing bias is applied to the first pseudorange. *Ground truth is at zero ordinate. Non-robust set inversion in thick blue, robust set inversion in red*

When using a nonrobust solver, inconsistencies between measurements can be detected when the solution set is empty. However, the measurement error may be too small to be detected, while nevertheless being large enough to make the computed location zone inconsistent with ground truth. This will be illustrated below.

In Fig. 8, a bias ramp is added to the first pseudorange of the set of six available pseudoranges. The nonrobust solution set (thick blue lines) remains consistent with ground truth until the bias reaches 18 m (a). With a measurement bias ranging from 18 to 23 m (b), ground truth is no longer consistent with the solution set, but there is no way of detecting this. This is the weakness of the nonrobust solver. Starting from a 24m bias, the solution set becomes empty (c), which proves that there is inconsistency between the measurements and the model.

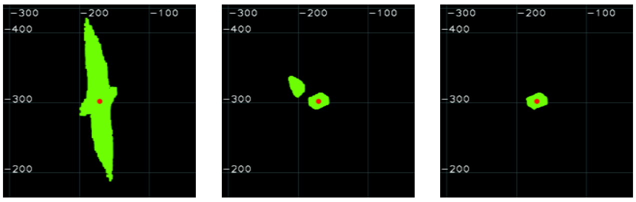

(a) no bias (b) 30 m bias (c) 50 m bias

Fig. 9 Horizontal projection of the 1-relaxed solution with one biased measurement. *Red dot is ground truth.*

Using a robust 1-relaxed solver, the presence of one wrong measurement does not compromise the integrity of the computed location zone. Changes in location zone bounds with respect to the pseudorange bias in Fig. 8 (thin red lines) can be explained in three phases. Up to a 19 m bias, a nonempty six-satellite solution can be computed. Since the solver is robust to one faulty measurement, all the five-satellite solutions are also included (Fig. 9a). The location zone gets tighter as the inconsistency grows. Starting from a 19 m bias, the presence of an erroneous measurement can be detected, as the six-satellite solution is the empty set. The solution set is thus composed only of five-satellite solutions. Figure 9b shows two nonempty five-satellite solutions. Finally, when the bias exceeds 50 m, only one five-satellite solution is nonempty, thus excluding the faulty measurement from the location zone computation (Fig. 9c). If necessary, the wrong measurement can be identified by testing the compatibility of the solution set with each measurement.

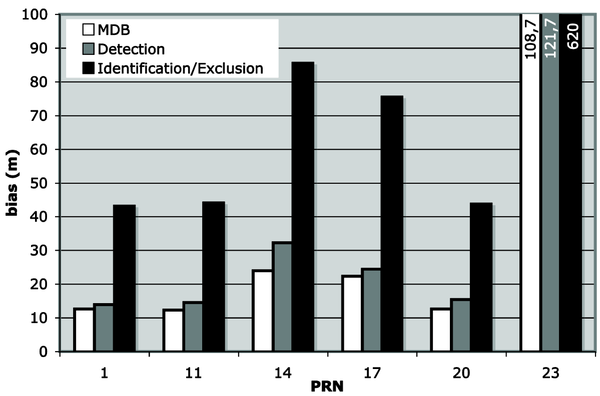

Fig. 10 MDB and fault detection and identification performance of the set-inversion method for each satellite at t=10s. *Values for satellite 23 have been truncated.*

The faults detected with the set-inversion method are consistent with minimal detectable biases. Results at a particular epoch are shown in Fig. 10. To allow comparison, we matched the error bounds choice with a $5 \cdot 10^{-5}$ false alarm probability and 10^{-3} probability of misdetection. MDB computations were done with standard analytical expression presented in Teunissen (1998).

Use of altitude information

When using a robust set inversion algorithm, the computed location zones tend to get wider. This is a direct consequence of considering the union of poorly-conditioned satellite-subset solutions. To counteract this phenomenon, more redundancy is needed. Since the visibility of GPS satellites may be reduced, especially in urban environments, other sources of information have to be used.

Altitude measurements can easily be obtained by the use of Digital Elevation Models (DEM) for land applications, analogous to altimeters used in avionics.

DEM fusion with GNSS pseudorange measurements can be done either by setting the prior searching box according to the measured altitude and its uncertainty, or by implementing a new constraint in the set inversion (Drevelle and Bonnifait 2009a).

We use a 25m horizontal grid resolution DEM with a 1m altitude precision covering the neighborhood of the lab (*BD Topo* charted by the French *Institut Géographique National - IGN*). An altitude contractor is applied to each box in the set inversion algorithm to enforce the altitude constraint.

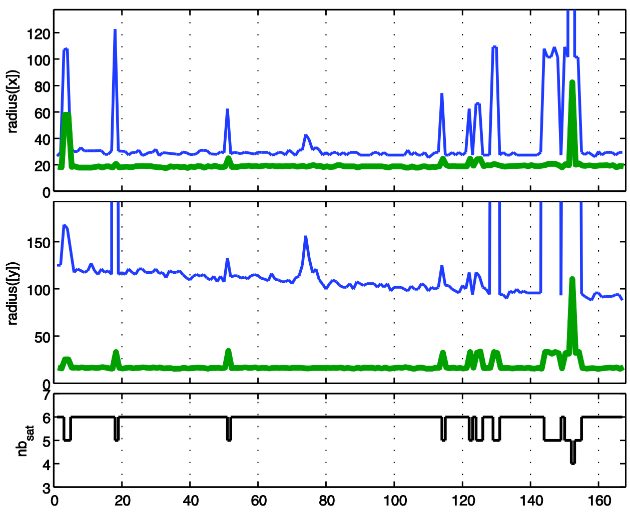

Fig. 11 1-relaxed location zone radius with *(thick green line)* and without *(blue line)* DEM information

In this trial. with the immunity to one erroneous measurement (RSIVIA with $q = 1$), the altitude information from the DEM reduces the horizontal location zone radius by a factor 5 on the y axis (Fig. 11).

The benefits of altitude information in reducing horizontal uncertainty are especially noticeable when few satellites are visible, or when robustness to a large number of faulty measurements is required. The altitude constraint provided by the DEM enables robust snapshot localization with as few as four satellites.

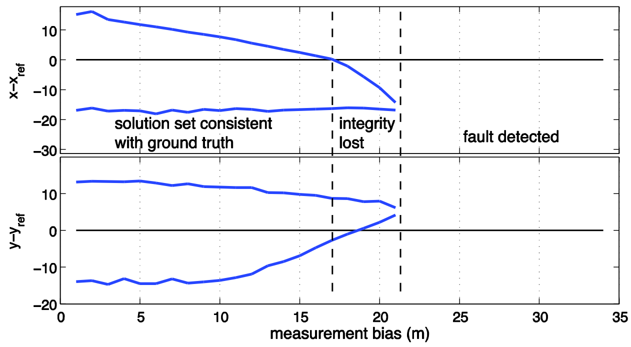

(a) Non-robust set inversion

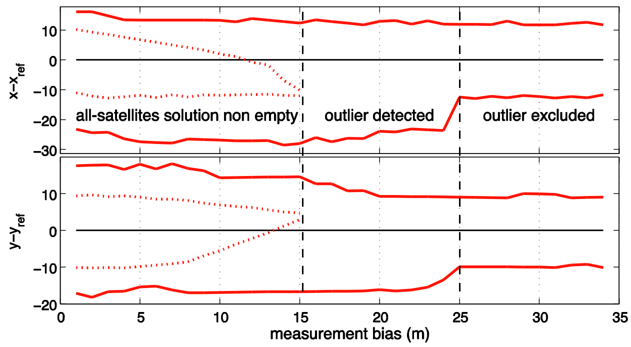

(b) Robust set inversion. Dotted lines are bounds of the set compatible with all measurements

Fig. 12 Location zone bounds with respect to ground truth, using DEM information. An increasing bias is applied on the first pseudorange.

Figure 12 shows the influence of a biased measurement on the horizontal position bounds, when merging DEM information with GPS pseudorange measurements. It is the same six-satellite dataset as in Fig. 10, allowing us to compare results with and without the use of a DEM. The nonrobust approach is little improved by the use of a DEM: Integrity is lost between 17 m and 21 m bias, while it was lost between 18 m and 23 m without the DEM information. Location zone is also a few meters tighter. A great improvement can be seen in the 1-relaxed solver behavior. The location zone always remains consistent with ground truth, since there is only one erroneous measurement, but it is tighter thanks to the added constraint, especially on the *y*-axis. The presence of an outlier is detected earlier, starting from a 16 m bias (19 meters without DEM). Moreover, the erroneous measurement is totally excluded from the solution after a 25m bias, where 50 m were necessary without DEM altitude information.

An experiment has also been conducted to compare the 1m resolution IGN DEM with a coarser DEM from the NASA's Shuttle Radar Topography Mission, with a 14m vertical accuracy. A ramp error was successively applied to each satellite in view, and the bias values for which error detection and identification occurred were recorded. Higher precision DEM not only allows detection of smaller biases (Fig. 13a), but it also significantly reduces the size of error needed to identify the faulty measurement (Fig. 13b).

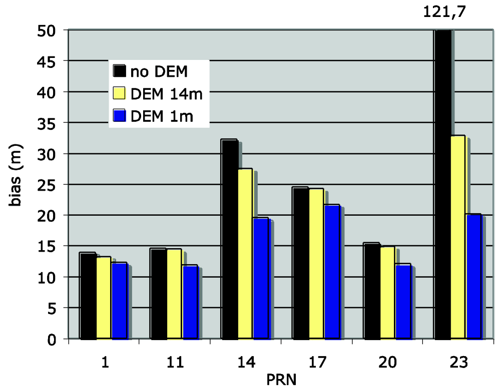

(a) Fault detection

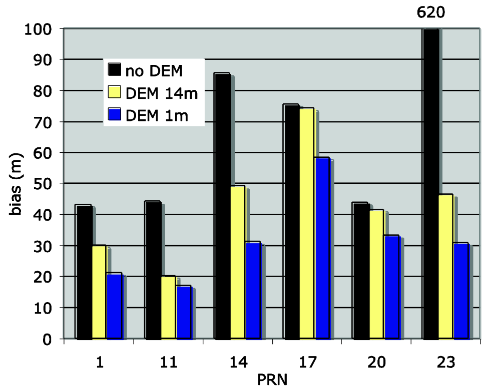

(b) Fault identification

Fig. 13 Influence of DEM precision on fault detection and identification

Maximum number of tolerated outliers

The maximum number of tolerated outliers has to be set before set-inversion. Several choices are available. If only satellite failures are considered, a reasonable approach is to set the maximum number of outliers to one. This approach can be used in an open sky environment, and it corresponds to the 'one fault at a time' hypothesis.

In urban areas, the risk of receiving simultaneous non-line-of-sight measurements is not negligible. Moreover, the number of visible satellites can be low. In this case, the number q of tolerated outliers can be set as a tradeoff between precision and integrity. The quality of the receiver and the antenna and their ability to reject reflected signals play a prominent part in the setting of q. For the *Septentrio PolaRx* and its polarized antenna, setting q=1 is a reasonable choice. With a low-end receiver with a patch antenna, it is common to receive three simultaneous wrong measurements in urban areas (Le Marchand et al. 2009). Setting q=3 ensures that a nonempty solution will exist most of the time.

Another approach can be based on the *Guaranteed Outlier Minimal Number Estimator* (Kieffer et al. 2000). The idea is to compute q-relaxed solutions with increasing values of q, until a nonempty solution is found. Robustness to undetectable errors can then be provided by adding a number of tolerated undetected errors to the value of q previously found.

Conclusion

A new method to characterize a location zone has been presented. It is based on robust set inversion using interval analysis. Bounds are set on measurements, taking error and risk into account. These bounded-error measurements translate into constraints in the location domain. Using interval analysis, the constraint satisfaction problem can then be solved, and a defined number of constraints can be relaxed in order to maintain solution integrity in the presence of outliers.

An experimental validation to compute location zones was carried out, using GPS pseudorange measurements corrected with EGNOS, and a Digital Elevation Model. It was implemented in real time as a parallelized C++ program. Results show that additional altitude information from the DEM enabled more precise positioning while tolerating GPS outliers, especially with a small number of visible satellites. Since each box in a subpaving can be processed independently of the others, the interval methods employed can be easily and efficiently parallelized to take advantage of the additional power of multi-core processors. The presented snapshot GPS-DEM robust location zone computation algorithm fails to provide a useful location zone when the number of pseudorange measurements becomes too low (with respect to the number of tolerated outliers). Future work will be focused on dynamic car positioning, using a kinematic vehicle model and embedded proprioceptive sensors. This will constrain the location zone, especially during GPS outages in difficult environments like urban canyons.

Aknowledgements The dataset and the reference trajectory used in this work were provided by Clément Fouque (*Heudiasyc UMR 6599, Université de Technologie de Compiègne*).

References

Baarda W (1968) A Testing Procedure for use in Geodetic Networks. Ned Geod Comm Publ on Geodesy, New series 2(5)

Bancroft S (1985) An algebraic solution of the GPS equations. IEEE T Aero Elec Sys 21(1):56–59

Brown RG (1992) A baseline GPS RAIM scheme and a note on the equivalence of three RAIM methods. Navigation

Chang TH, Wang LS, Chang FR (2009) A Solution to the Ill-Conditioned GPS Positioning Problem in an Urban Environment. IEEE T Intell Transp 10(1):135–145

Drevelle V, Bonnifait P (2009a) High integrity GNSS location zone characterization using interval analysis. In: Proceedings of ION GNSS 2009, pp 2178–2187

Drevelle V, Bonnifait P (2009b) Integrity Zone Computation using Interval Analysis. In: Proceedings of the European Navigation Conference (GNSS 2009)

Feng S, Ochieng W, Walsh D, Ioannides R (2006) A measurement domain receiver autonomous integrity monitoring algorithm. GPS Solut 10(2):85–96

Fouque C, Bonnifait P (2008) Tightly-coupled GIS data in GNSS fix computations with integrity testing. Int J Intell Inf Database Syst 2(2):167–186

Gutmann J, Marti L, Lammel G (2009) Multipath Detection and Mitigation by Means of a MEMS Based Pressure Sensor for Low-Cost Systems. In: Proceedings of the 22nd International Meeting of the Satellite Division of The Institute of Navigation, pp 2077–2087

Hewitson S, Wang J (2007) GNSS Receiver Autonomous Integrity Monitoring with a Dynamic Model. J Navig 60(2):247–263

Huber PJ (1964) Robust estimation of a location parameter. Ann Math Stat 35(1):73–101

Jaulin L (2009) Robust set-membership state estimation; application to underwater robotics. Automatica 45(1):202–206

Jaulin L, Walter E (1993) Set inversion via interval analysis for nonlinear bounded-error estimation. Automatica 29(4):1053–1064

Jaulin L, Kieffer M, Braems I, Walter E (2001a) Guaranteed Nonlinear Estimation Using Constraint Propagation on Sets. Int J Control 74(18):1772–1782

Jaulin L, Kieffer M, Didrit O, Walter E (2001b) Applied Interval Analysis. Springer-Verlag

Jaulin L, Kieffer M, Walter E, Meizel D (2002) Guaranteed Robust Nonlinear Estimation with Application to Robot Localization. IEEE T Syst Man Cy C 32(4):374–382

Kaplan E, Hegarty C (2006) Understanding GPS: Principles and Applications Second Edition. Artech House Publishers

Kieffer M, Jaulin L, Walter E, Meizel D (2000) Robust Autonomous Robot Localization Using Interval Analysis. Reliable Computing 6(3):337–362

Le Marchand O, Bonnifait P, Ibanez-Guzmán J, Bétaille D, Peyret F (2009) Characterization of GPS multipath for passenger vehicles across urban environments. ATTI dell'Istituto Italiano di Navigazione 189:77–88

Leick A (2004) GPS satellite surveying, Third edition.Wiley

Li J, Taylor G, Kidner DB (2005) Accuracy and reliability of map-matched GPS coordinates: The dependence on terrain model resolution and interpolation algorithm. Comput Geosci 31(2):241–251

Meizel D, Leveque O, Jaulin L, Walter E (2002) Initial localization by set inversion. IEEE T Robotic Autom 18(6):966–971

Moore RE (1966) Interval analysis. Prentice Hall

Röhrig C, Müller M (2009) Indoor location tracking in non-line-of-sight environments using IEEE 802.15.4a wireless network. In: Conference Proceedings of IROS09, pp 552–557

Salzmann M (1991) MDB: a design tool for integrated navigation systems. Journal of Geodesy 65(2):109–115

Schroth G, Ene A, Blanch J, Walter T, Enge P (2008) Failure Detection and Exclusion via Range Consensus. In: Proceedings of the European Navigation Conference

Schubert A (2006) Comparison of Solution Separation Method with Parity Space Methods. In: Proceedings of ENC-GNSS 2006

Teunissen PJG (1990) Quality Control in Integrated Navigation Systems. IEEE Aerosp Electron Syst Mag 5(7):35–41

Teunissen PJG (1998) Minimal Detectable Biases of GPS Data. Journal of Geodesy, 72:236–244

Walter T, Enge P (1995) Weighted RAIM for precision approach. In: Proceedings of ION GPS, Institute of Navigation, pp 1995–2004